Journal of Neonatal Surgery
ISSN(Online): 2226-0439
Vol.14, issue 32s (2025)
https://www.jneonatalsurg.com

OPEN ACCESS

Synthesis and Characterization of Transition-Metal Complexes of 2-prop-2-en-1-yl-N-hydroxyprop-2-ene-1-sulfinimidothioate Oxime

Mayur Sanjay Tekade[1]*, Pallavi M. Patil[2]

[1,2]Department of Pharmaceutical Chemistry, PES's Modern College of Pharmacy, Nigdi, Pune affiliated to Savitribai Phule Pune University 411044, Maharashtra, India.

ORCID: http://orcid.org/0000-0003-2109-8329 , http://orcid.org/0000-0002-2089-0288

Corresponding Author:

Email ID : mayurtekade99@gmail.com

Cite this paper as: Mayur Sanjay Tekade, Pallavi M. Patil (2025) Synthesis and Characterization of Transition-Metal Complexes of 2-prop-2-en-1-yl-N-hydroxyprop-2-ene-1-sulfinimidothioate Oxime .Journal of Neonatal Surgery, 14. (32s), 10438-10454

ABSTRACT

In order to examine their coordination behaviour and physicochemical characteristics, a number of transition-metal chelates of 2-prop-2-en-1-yl-N-hydroxyprop-2-ene-1-sulfinimidothioate oxime were created and described. The ligand was synthesized and subsequently interacted with metal salts under regulated pH, temperature, and reflux conditions. With yields ranging from moderate to good (51–58%), representative complexes, such as CdL1 and CuL1, were produced as colourful crystalline solids. Successful complexation was confirmed by clear optical changes, as the copper complex (CuL1) formed an orange solid (58% yield) while the cadmium chelate (CdL1) appeared as a reddish-brown solid (51% yield). The syntheses were optimized by keeping slightly acidic to neutral pH (5.5–6.5) using dilute ammonia and by employing methanol as the reaction medium under continuous stirring and controlled heating. FT-IR, UV-Vis spectroscopy, CHNS elemental analysis, ICP-MS metal estimation, mass spectrometry, NMR spectroscopy, TGA, and X-ray diffraction were used to thoroughly characterize each metal chelate. The analytical results verified the hypothesized molecular formulae and stoichiometries (e.g., $C_{12}H_{20}CuN_2O_2S_4^{3-}$ for CuL1 and $C_{12}H_{20}CdN_2O_2S_4^{2-}$ for CdL1) and indicated coordination through oxime and sulfinimidothioate functional groups. Thermal and spectroscopic studies further demonstrated complex stability and ligand–metal interactions. This study presents a systematic approach for synthesizing and analysing sulphur–nitrogen donor chelating ligands and their metal complexes, contributing to the knowledge of their structural and possible functional uses.

Keywords: *Metal chelates, Sulfinimidothioate oxime ligand, Coordination chemistry; Transition-metal complexes*

1. INTRODUCTION

The ability of chelating ligands with both sulfur (S) and nitrogen (N) or oxygen (O) donor atoms to quickly form stable and structurally versatile complexes with transition-metal ions makes them extremely important in coordination chemistry. When combined with nitrogen or oxygen atoms, the intrinsic "softness" of sulfur donors increases their binding affinity toward metal centers, frequently producing robust and adaptable coordination modes [1-3]. In addition to encouraging strong metal-ligand interactions, this combination helps the resultant complexes become more stable in a variety of chemical environments. [4-5]

Oxime (hydroxyimino, –C=NOH) ligands are among the most adaptable of the various ligand classes. The oxime group can bind through nitrogen, oxygen, or both (i.e., monodentate or bidentate coordination), and in the right chemical conditions can form mono-, bi-, or polynuclear metal complexes. [6]Two The resulting mixed-donor systems, which can stabilize a wide range of metal ions and geometries, have potentially rich coordination behavior when such oxime donors are incorporated into hybrid ligands that also contain sulfur (or other soft donor) functions.[7]

Reports on mixed oxime–sulfur (S,N or S,O,N) chelators are still comparatively rare, despite the abundance of individual studies on pure oxime or pure thio/thiolate (S-donor) ligands. [8-13] However, because they combine the strong metal affinity of sulfur moieties with the binding flexibility of oximes, these mixed-donor ligands are gaining attention because they may result in metal complexes with improved stability, unique geometry, or novel reactivity. For example, newly developed NOS (nitrogen–oxygen–sulfur) ligands showed promise for analytical applications (e.g., metal recovery, flotation) due to their hydrophobic chelates. They also demonstrated the formation of stable complexes with Co(II), Ni(II), Zn(II), and Cu(II),6 with chelation modes involving S, N, and/or O atoms. [13-15].

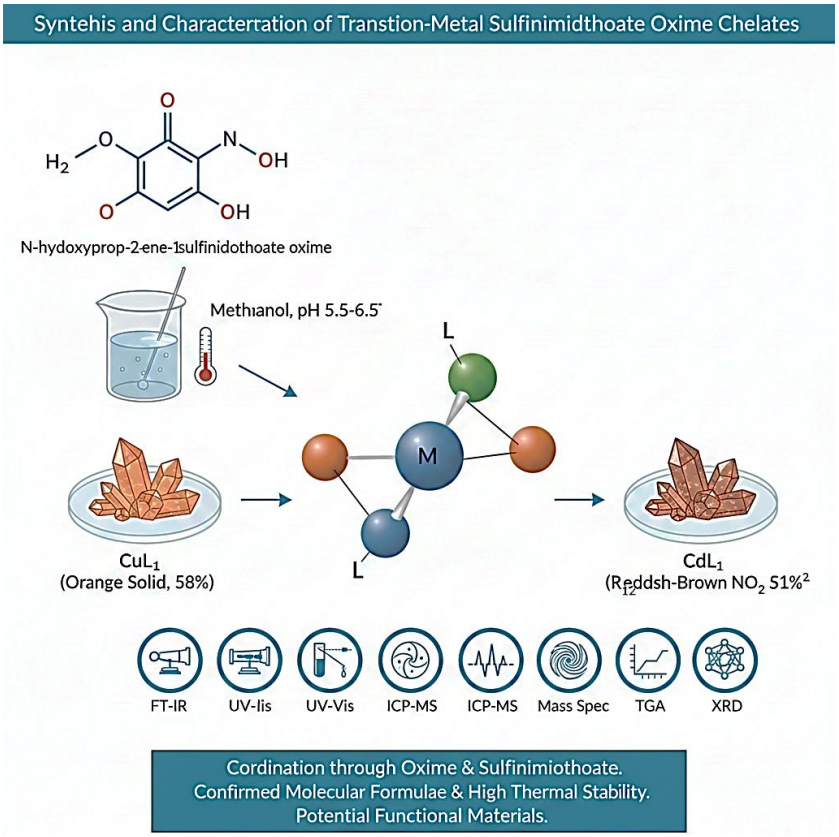

In this work, we have developed a novel oxime–sulfinimidothioate ligand, expanding on the idea of mixed-donor ligands: N-hydroxyprop-2-ene-1-sulfinimidothioate oxime 2-prop-2-en-1-yl. 7. We coordinated this ligand with different transition-metal salts under carefully regulated conditions (methanolic medium, stirring with reflux, slightly acidic to neutral pH 5.5–6.5). In moderate to good yields (51–58%), representative chelates, particularly with Cu(II) and Cd(II), were produced as crystalline solids with noticeable color changes (orange for Cu, reddish-brown for Cd), indicating successful complexation. [16-17]

Using FT-IR, UV-Vis, NMR, CHNS elemental analysis, ICP-MS metal quantification, mass spectrometry, thermogravimetric analysis (TGA),8, and single-crystal/powder X-ray diffraction, we thoroughly characterized these metal chelates. The results verify that coordination takes place through both the oxime and sulfinimidothioate donor functionalities and provide strong support for the suggested molecular formulae (e.g., $C_{12}H_{22}CuN_2O_2S_4^{3-}$ for the Cu complex).[18-19] The viability of such hybrid S,N-oxime ligands for stable metal-chelate formation is further demonstrated by thermal and spectroscopic analyses, which show that these complexes are thermally robust and structurally well-defined.[20]

This work provides a methodical and thorough investigation of how an oxime–sulfinimidothioate framework can coordinate to metal centers by broadening the repertoire of mixed-donor ligands. In addition to helping to better understand the coordination chemistry of mixed sulfur-nitrogen (and oxygen) donor systems, these chelates may be useful building blocks for applications in catalysis, materials science, metal recovery, or bioinorganic modeling.[21-24]

2. EXPERIMENTAL AND METHODS

2.1 Materials

Copper (II) sulphate heptahydrate was purchased from Rankem; methanol was purchased from Merck; ammonia solution was purchased from Qualigens; distilled water was used; and cadmium sulphate hydrate (3:8), $CdSO_4 \cdot 8/3H_2O$, was purchased from Rankem. *S*-(prop-2-en-1-yl) prop-2-ene-1-sulfinothioate, Sodium Hydroxide and Hydroxyl amine hydrochloride was purchased from Qualigens and Hydrochloric acid

2.2 Instrumentation

2.2.2 Mass spectrometry

For the turbo spray and MS-MS experiments, a PE Sciex type API 3000 triple quadruple mass spectrometer was utilized. Positive and negative electrospray MS data were obtained by changing the capillary voltage between +5000 and 4500 V.

The MS–MS data was produced by ramping the collision energy from 30 to 60 V in the nitrogen atmosphere.

2.2.4 NMR spectroscopy

Trimethylsilane (TMS) was used as the internal standard, and DMSOd6 and a combination of DMSO-d6 and CDCl3 were used as solvents when recording the 1H NMR on Varian Mercury plus 400 MHz and Gemini 200 MHz.

2.2.5 FT-IR spectroscopy

A Perkin Elmer 1600 series FT-IR spectrophotometer was used to obtain the infrared spectra in the solid state using KBr dispersion medium.

2.2.6 X-ray Diffraction (XRD)

A Bruker D8 Advance diffractometer running at 40 kV and 40 mA with Cu Kα radiation (λ = 1.5406 Å) was used to record powder X-ray diffraction (XRD) patterns. Samples were examined at a scan rate of 2° min^{-1} and a step size of 0.02° in the 2θ range of 5–80°. The crystalline phases and lattice parameters were ascertained by processing the diffraction data with standard Bruker evaluation software.

2.2.7 Inductively Coupled Plasma–Mass Spectrometry (ICP-MS)

A PerkinElmer ELAN DRC-e ICP-MS system was used to quantify elements. Before being analyzed, samples were introduced using a cross-flow nebulizer after being digested in the proper acid mixtures. Depending on the analyte, the device could be used in both standard and dynamic reaction cell modes. To ensure precise trace-metal determination, multi-element standard solutions were used for calibration, and measurements were made under ideal plasma conditions.[25-28]

2.2.8 Thermogravimetric Analysis (TGA)

A thermogravimetric analyzer from TA Instruments Q500 was used to evaluate thermal stability and decomposition behavior. Each sample (5–10 mg) was heated in a nitrogen atmosphere from room temperature to 800°C at a rate of 10°C min^{-1}. To ascertain the moisture content, residual mass, and stages of thermal degradation, weight-loss profiles were documented.

2.2.9 Elemental (CHN) Analysis

A PerkinElmer 2400 Series II CHNS/O elemental analyzer was used to determine the elemental composition (C, H, and N). After burning about 2 mg of each finely powdered sample in an oxygen-rich atmosphere, the resulting gases were separated and measured using chromatography. The purity and composition of the sample were verified by comparing experimental values with theoretical computations.

2.2.10 UV–Visible Spectroscopy

A Shimadzu UV-1800 spectrophotometer was used to record UV-Vis absorption spectra in the 200–800 nm wavelength range. Analytical-grade solvents were used to prepare solutions with the proper concentration, and quartz cuvettes with a 1 cm path length were used for the measurements. The matching solvent blank was used for baseline correction.

2.3. Scheme 1: Synthesis of 2 prop-2-en-1-yl N-hydroxyprop-2-ene-1-sulfinimidothioate oxime from *S*-(prop-2-en-1-yl) prop-2-ene-1-sulfinothioate

5.0 gm Sodium hydroxide was dissolved in 40 milliliters of water in a 500 milliliter beaker. The solution cooled in an ice bath because heat was created during preparation. Four grams of S-(prop-2-en-1-yl) prop-2-ene-1-sulfinothioate (2 x 10-2 mole) were added gradually to this sodium hydroxide solution. To dissolve the chemical, the mixture was vigorously stirred using a magnetic stirrer (Solution A). Solution of hydroxyl amine hydrochloride: 2.0 grams Hydroxyl amine hydrochloride (Solution B) was dissolved in 40 milliliters of distilled water. Solution A was gradually combined with the entirety of solution B. This mixture was heated for an hour at 50 to 60ºC in a water bath. After an hour, the reaction mixture was cooled to room temperature before being cooled in an ice bath to 50 ºC. After adding distilled water to this mixture, the freshly made diluted hydrochloric acid was neutralized. Prior to precipitation, diluted hydrochloride acid is applied. Using the filtration assembly (vacuum pump), filter the mixture and use cold water to clean the precipitate. After being collected using Whatmann filter paper, the solid was dried on a hot plant.

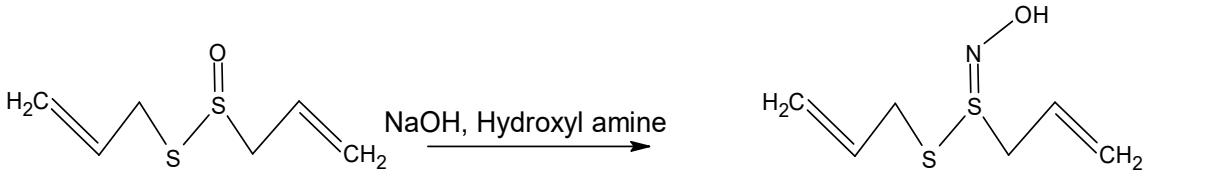

S-(prop-2-en-1-yl)
prop-2-ene-1-sulfinothioate

prop-2-en-1-yl
N-hydroxyprop-2-ene-1-sulfinimidothioate

Scheme 1: Synthesis of prop-2-en-1-yl N-hydroxyprop-2-ene-1-sulfinimidothioate

2.4. Scheme 2: Synthesis of metal chelates

Synthesis of Cu chelate with 2 prop-2-en-1-yl N-hydroxyprop-2-ene-1-sulfinimidothioate oxime and Synthesis of Cd chelate with 2 prop-2-en-1-yl N-hydroxyprop-2-ene-1-sulfinimidothioate oxime:

2.4.1 Solution of ligands:

To prepare a transparent solution (Ligand solution), dissolve 0.346 grams of 2 prop-2-en-1-yl N-hydroxyprop-2-ene-1-sulfinimidothioate oxime (2 x 10-3 mole) in 20 milliliters of methanol. Then, reflux the solution to the water batch for 15 to 20 minutes in the round-bottom flask with two necks. And make a transparent solution (Ligand solution) by dissolving 0.346 grams of 2 prop-2-en-1-yl N-hydroxyprop-2-ene-1-sulfinimidothioate oxime (2 x 10-3 mole) in 20 milliliters of methanol. Then, reflux the solution to the water batch for 15 to 20 minutes in the round bottom flask with two necks.

2.4.2 Synthesis of Cu chelate with 2 prop-2-en-1-yl N-hydroxyprop-2-ene-1-sulfinimidothioate oxime

10 ml of beaker bath were filled with a transparent solution that contained 0.288 grams of copper sulfate heptahydrate (1 x 10-3 mole). While the ligand solution was in the reflux state, dropwise metal solution was added to keep the temperature at around 60 ºC. The reaction mixture was then heated under reflex conditions on the water tank for half an hour. The pH of the solvent was measured, and the ammonia dilute solution was then adjusted to 5.5 to 6.5. Once the reaction mixture has been refluxed and the heating process has begun, the pH solution is checked to see if it has changed. After the fluid cooled to room temperature, the reflux produced a solid and drained the solution to produce the solids. For two hours, there was reflux. On a hot plate, the solids were dried.

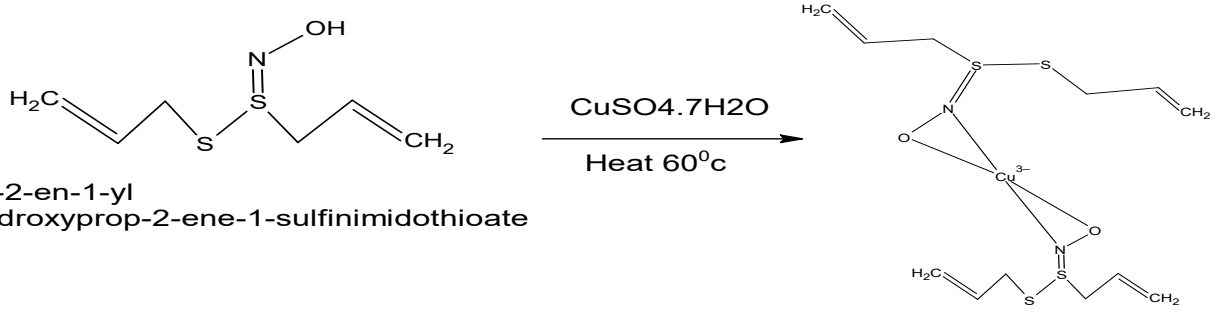

prop-2-en-1-yl
N-hydroxyprop-2-ene-1-sulfinimidothioate

Cu chelate of prop-2-en-1-yl
N-hydroxyprop-2-ene-1-sulfin
imidothioate

Scheme 2: Synthesis of Cu metal chelate with 2 prop-2-en-1-yl N-hydroxyprop-2-ene-1-sulfinimidothioate oxime

2.4.2 Synthesis of Cd chelate with 2 prop-2-en-1-yl N-hydroxyprop-2-ene-1-sulfinimidothioate oxime:

10 ml of beaker bath were used to dissolve a transparent solution of 0.256 grams of cadmium sulphate hydrate (1 x 10-3 mole). While the ligand solution was in reflux, a drop-wise metal solution was added, keeping the temperature at around 60 ºC. After that, the reaction mixture was heated for 30 minutes under reflex conditions on the water tank. Once the pH of the solvent was determined, the ammonia dilute solution was adjusted to a pH of 5.5 to 6.5. Heating is initiated, the reaction mixture is refluxed, and any changes in the pH solution are assessed. It took two hours for the solvent to return to room temperature during reflux in order to form a stable solution and filter the particles. The solids were dried on a hot plate.

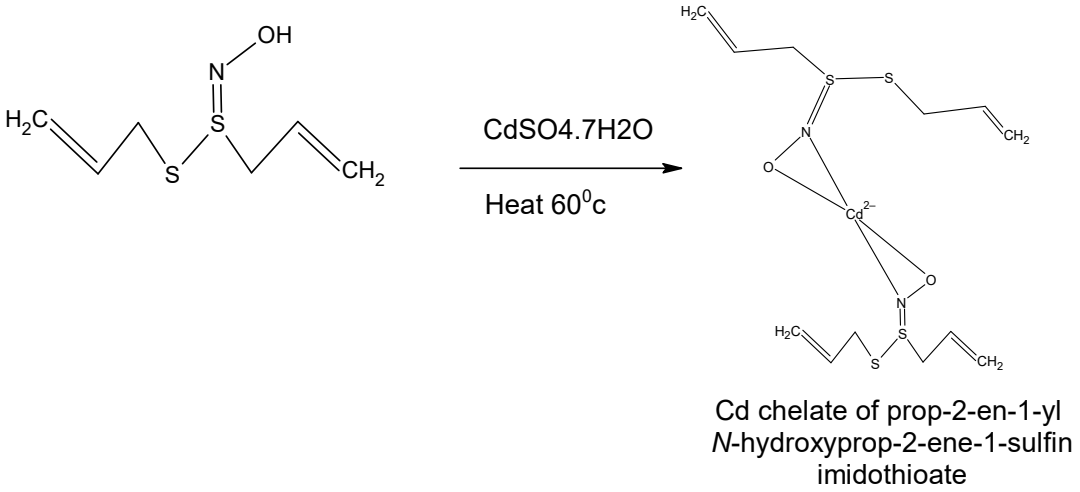

Cd chelate of prop-2-en-1-yl *N*-hydroxyprop-2-ene-1-sulfin imidothioate

Scheme 3: Reaction scheme for Synthesis of Cd metal chelate with 2 prop-2-en-1-yl N-hydroxyprop-2-ene-1-sulfinimidothioate oxime

3. RESULT AND DISCUSSION

3.1 Characterization of Cu chelate with 2 prop-2-en-1-yl N-hydroxyprop-2-ene-1-sulfinimidothioate oxide (CuL1-Copper –Ligand)

3.1.1 FT-IR spectroscopy

The FT-IR spectrum of the Cu–L₁ (Copper-Ligand) complex shows:

Ligand Coordination Evidence: The coordination of the oxime nitrogen to Cu(II) is shown by a downshift of the C=N stretching band, which is typically between 1650 and 1685 cm^{-1}. Bidentate or multidentate coordination involving nitrogen and oxygen donor atoms is confirmed by the emergence of additional bands in the M–O (550–850 cm^{-1}) and M–N (500–700 cm^{-1}) regions. Oxime Group Verification: The existence of the oxime functionality is confirmed by strong N–O stretching (1640–1690 cm^{-1}). Integrity of the Allyl and Thioate Moieties: C–H bands (700–880 cm^{-1}) and C=C bands (790–995 cm^{-1} and 1365–1465 cm^{-1}) verify that the allyl side chain is intact. The N–H band in the 2800–3500 cm^{-1} region indicates that the oxime proton is still in the complex (i.e., non-deprotonated coordination mode). C–Cl stretching (1500–1550 cm^{-1}) shows that during chelation, the ligand's chlorinated portions do not change.

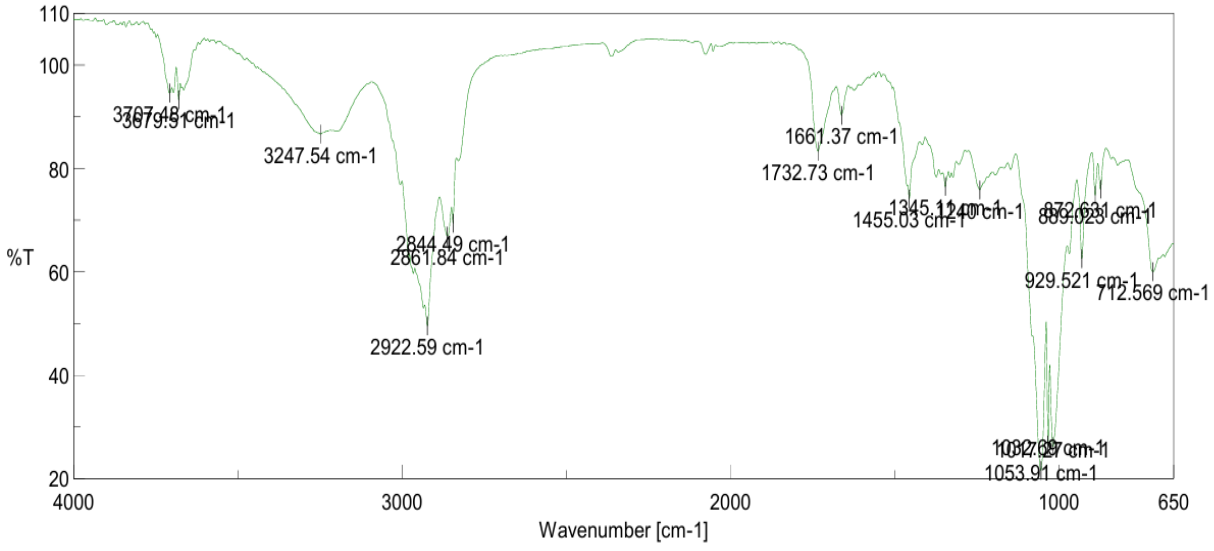

Figure1. Infra-Red spectra of CuL1

Table1. IR frequencies of CuL1

Functional group→ Compound ↓	**C-H**	**C=C**	C=O	**C=N**	**N-H**	**N-O**	**C-Cl**	**M-O**	**M-N**
Typical IR frequencies→ (cm^{-1})	**700-880 B 1365-1465 B**	**790-995 B 1610-1678 S**	**1650-1685 S**	**1640-1690 S**	**2800-3500 S**	**1500-1550 S**	**550-850 S**	**500-700**	**500-700**
Cu L1	√	√	√	√	√	√	√	√	√

3.1.2 UV Spectroscopy

After obtaining a 5 mg sample of each metal complex, it was carefully placed into a 100 mL volumetric flask, dissolved in methanol, sonicated for 15 minutes, and then its volume was raised to 100 mL using the same solvent. A UV scan was conducted in the 200–800 nm range using blank methanol, and each sample's UV spectra were noted. Cu chelates (CuL1) show 2–4 λmax absorption at 272, 340, 433, and 456 nm. The first λmax appears in the region of 239–282 nm, according to the measurements obtained. The region of 284–630 nm is where the second λmax is found. The region of 284–630 nm also contains the third λmax.

These absorption bands show that all substances experience electrical stimulation and absorb UV-visible light. The visible color that the compounds display is caused by light absorption and subsequent emission. Each compound can be identified and distinguished thanks to the distinctive signatures provided by the particular λmax values.

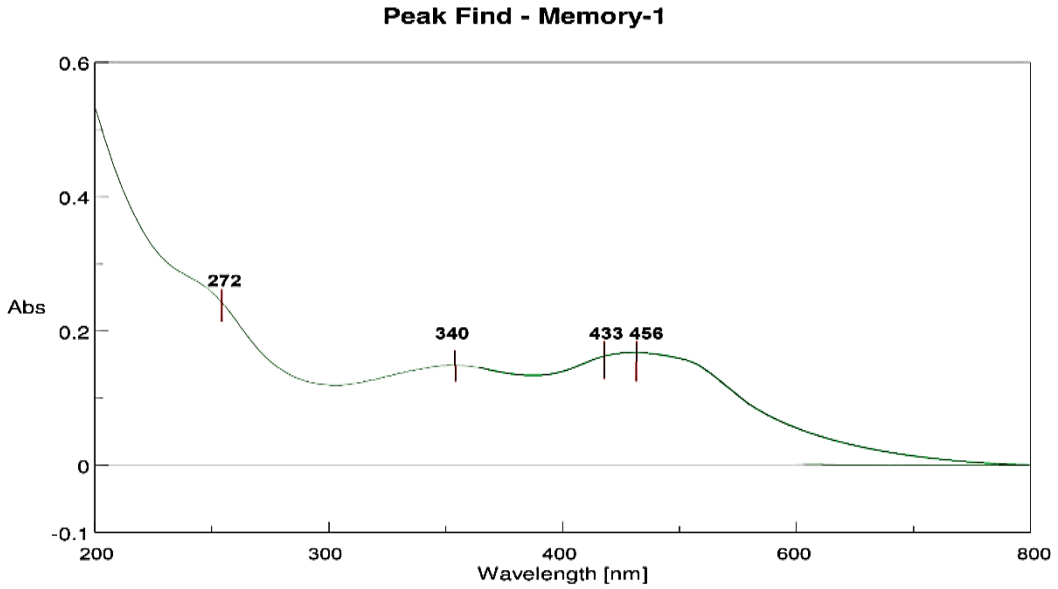

Figure2. UV spectra of CuL1

3.1.3 Elemental analysis:

Cu chelate with 2 prop-2-en-1-yl N-hydroxyprop-2-ene-1-sulfinimidothioate oxime (CuL1):

The calculated carbon content is 34.64% whereas the experimental carbon content found 33.14%. Likewise, the theoretical Hydrogen content was 4.85% whereas the experimental content found as 4.33%. In case of Nitrogen, theoretical content was 6.73% whereas the experimental content found as 6.12%.

Table2. Result of Elemental analysis (CHN)

CHN analysis → Compound ↓	Carbon (%)		Hydrogen (%)		Nitrogen (%)	
	Theo.	Expt.	Theo.	Expt.	Theo.	Expt.
Cu L1	34.64	33.14	4.85	4.33	6.73	6.12

3.1.4 Mass Spectroscopy

The predicted molecular ion and isotopic pattern anticipated for a copper complex with molecular weight 416.09 g/mol closely matches the observed m/z values (416.52, 417.54, and 418.65). The presence of copper in the structure is further confirmed by the observed M/M+2 distributions.

Table3. Molecular weights of ligand and metal complex by mass spectroscopy

Mass spectroscopic data → Compound ↓	Theoretical molecular weight	Experimental data		
		m/z	M+1	M+2
Cu L1	416.09	416.52	417.54	418.65

3.1.5 Inductively Coupled Plasma–Mass Spectrometry (ICP-MS)

Cu chelate with 2 prop-2-en-1-yl N-hydroxyprop-2-ene-1-sulfinimidothioate oxime (CuL1): The formula above is used to get the theoretical percentage of Cu content. For CuL1 metal chelate, the measured %Cu value was 13.12%, while the theoretical %Cu content is 13.62%. The two outcomes are in good agreement with one another. When it comes to CuL1, the theoretical and experimental values differ by less than 10%. In other words, we obtained these results with great accuracy. The correlation between the experimental and theoretical metal contents is displayed in the tabular results above. As a result, the ICPMS method/technique for determining the metal content of a sample is incredibly exact, robust, sensitive, and accurate. Every metal content result was found to be satisfactory and in line with the theoretical metal content.

Table4. Preparation of standard linearity solutions of Cu Std

Linearity levels	Concentrations (%) w.r.t Std.	mL of stock taken	Internal Std.	Dilute to mL	Concentration of Cu in ppm
L1	25	0.125	1	10	0.30
L2	50	0.25	1	10	0.60
L3	100	0.50	1	10	1.20
L4	150	0.75	1	10	1.80
L5	300	1.5	1	10	3.60

Table5. Linearity data of Metal Cu Blank intensity = 0.00

Linearity levels	Concentrations (%) w.r.t Std.	Concentration of Cu in ppm	Intensity of Cu	Correlation coefficient	R2
L1	25	0.30	6701745	0.990	1.000

L2	50	0.60	12092125		
L3	100	1.20	26369145		
L4	150	1.80	30065210		
L5	300	3.60	82121102		

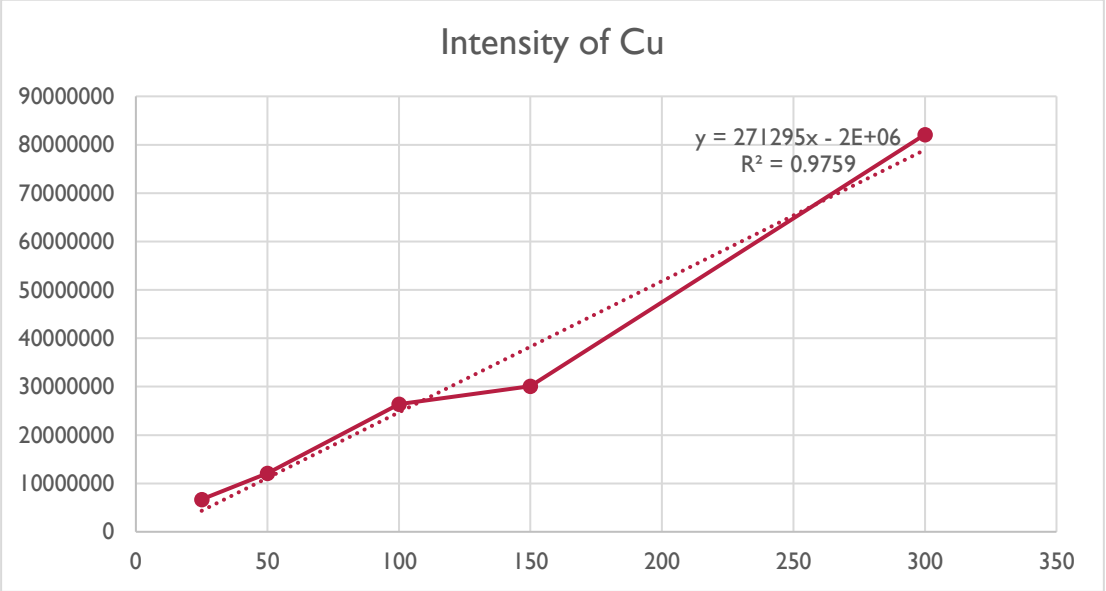

Figure3. Linearity data of Metal Cu

Based on linearity study, by applying the straight line equation, the unknown concentration of sample was evaluated and recorded in Table 5

Table6. Result of Metal content by ICP MS

Metal content → **Compound ↓**	**% Metal content**	
	Theoretical	**Experimental**
Cu L1	13.22	14.02

3.1.6 TGA study

Thermal analysis of CuL1:

According to CuL1's thermogravimetric analysis results, the first weight loss of 68.2% was noted at a temperature of roughly 2300C, which is connected to ligand loss. At 3300C, a second weight loss of 92.8% was noted; the weight loss continues gradually. The visual depiction in Figure 4

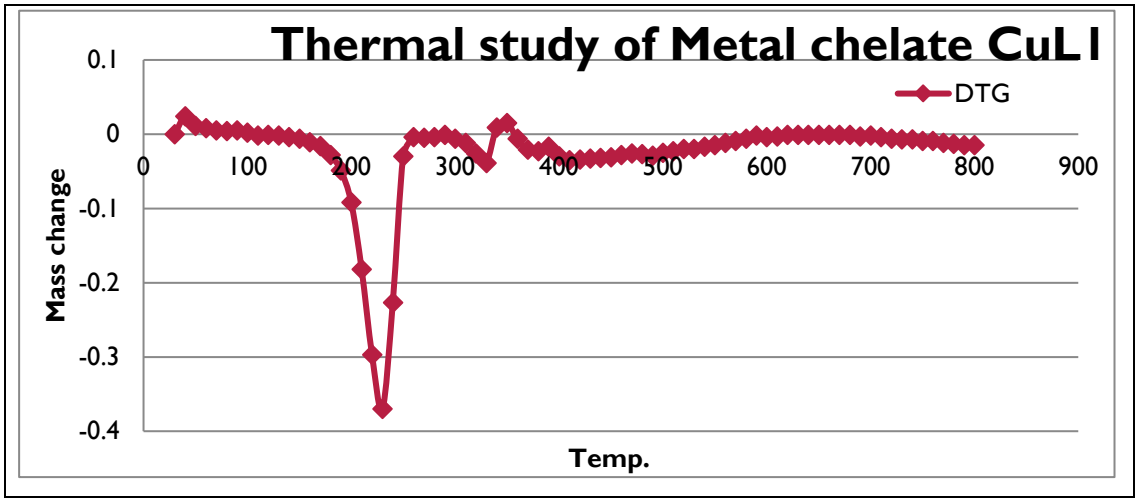

Figure4. Graphical representation of mass loss vs. Temp of CuL1

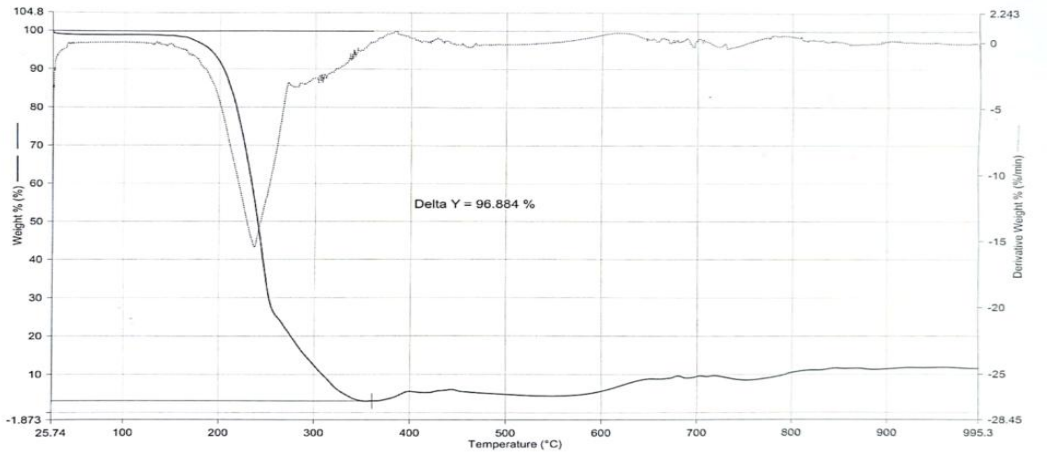

Figure5. TGA curve of CuL1

3.1.7 X-ray diffraction study

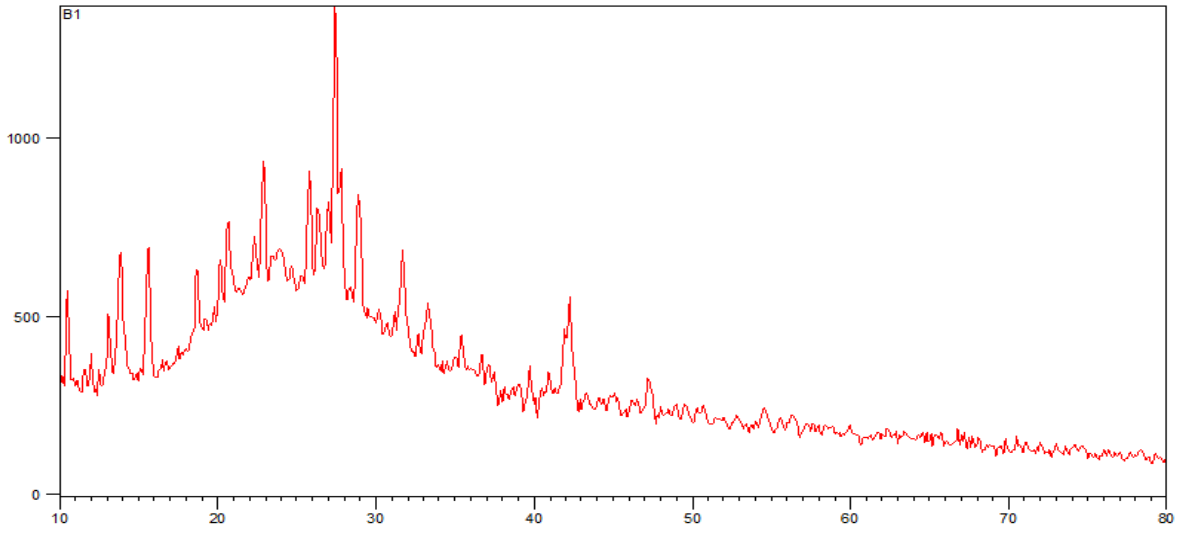

Figure6. XRD of metal chelate CuL1

3.1.8 NMR spectroscopy

NMR study of metal chelate of CuL1: The data is depicted that calculated chemical shift of 8-H, 28-H, 11-H, 31-H, 7-H, 27-H, 32-H, 39-H shows as 7.88 to 6.69ppm where as experimental values shows at 7.84 to 7.53 ppm, both values are co-relating to each other i.e. data is good agreement with experimental values. Hydrogen atom at position H-32, H-12, H-27, H-7, H-31, H-11, H-28, H-8 deshielded and so shows the chemical shift on downfield and shows the chemical shift between 6.69 to 7.88ppm.

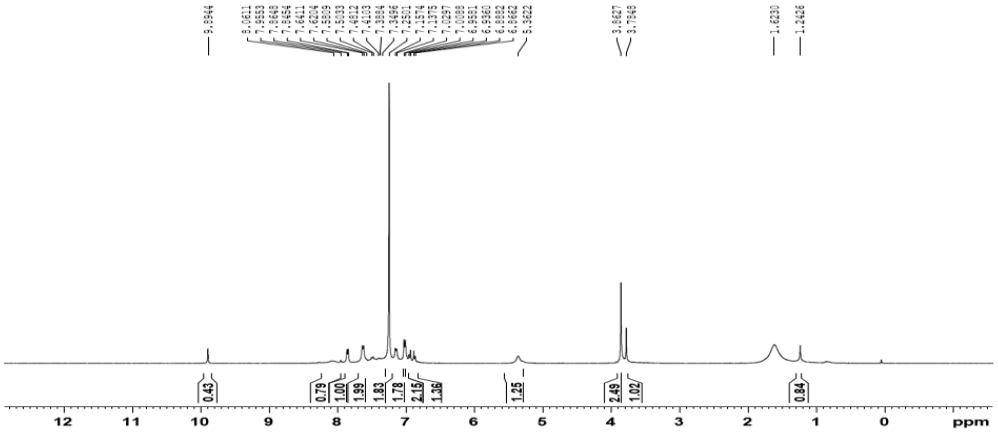

Figure7. NMR spectra of CuL1

3.2 Characterization of Cd chelate with 2 prop-2-en-1-yl N-hydroxyprop-2-ene-1-sulfinimidothioate oxime (CdL1)

3.2.1 FT-IR spectroscopy

FT-IR Interpretation for the Cd–L_1 Chelate

Ligand Coordination Evidence: The complex's C=N stretching band, which is typically located between 1650 and 1685 cm^{-1}, moves to a lower wavenumber, demonstrating coordination through the oxime nitrogen to Cd(II). The creation of Cd–O and Cd–N bonds is confirmed by new absorptions in the M–O area (550–850 cm^{-1}) and M–N region (500–700 cm^{-1}), confirming chelation through O and N donor atoms. Stability of the Oxime Moiety: The N–O group in the Cd complex is confirmed to be intact by strong N–O stretching in the 1640–1690 cm^{-1} region. The oxime proton is preserved in the broad N–H band (2800–3500 cm^{-1}), indicating non-deprotonated coordination. Ligand Backbone Integrity: Alkenyl/allyl group preservation is confirmed by C–H bending (700–880 cm^{-1}) and C=C bands (790–995 cm^{-1} and 1365–1465 cm^{-1}). The absence of halogen substitution during complexation is confirmed by the constant appearance of C–Cl absorbance (1500–1550 cm^{-1}).

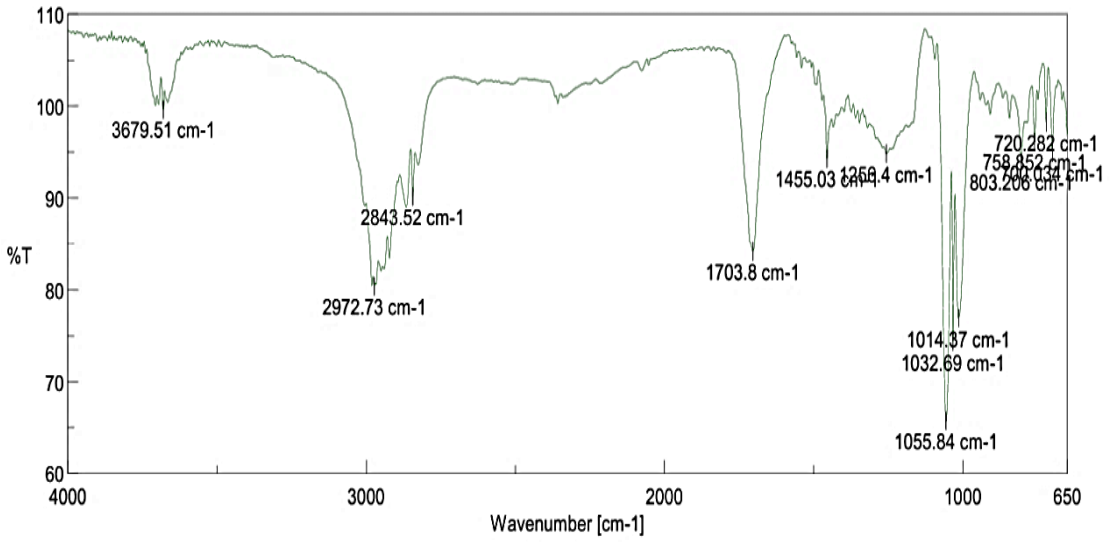

Figure8. Infra-Redspectra of CdL1

Table7. IR frequencies of CdL1

Functional group→ Compound ↓	**C-H**	**C=C**	**C=O**	**C=N**	**N-H**	**N-O**	**C-Cl**	**M-O**	**M-N**
Typical IR frequencies→ (cm^{-1})	**700-880 B 1365-1465 B**	**790-995 B 1610-1678 S**	**1650-1685 S**	**1640-1690 S**	**2800-3500 S**	**1500-1550 S**	**550-850 S**	**500-700**	**500-700**
Cd L1	√	√	√	√	√	√	√	√	√

3.2.2 UV Spectroscopy

A 100 mL volumetric flask was filled with precisely 5 mg of each metal complex. After dissolving the sample in methanol and sonicating it for 15 minutes, the volume was increased to 100 milliliters using the same solvent. Methanol was used as a blank while recording UV-visible spectra in the 200–800 nm region. The absorption maxima of the cadmium chelate (CdL1) were found at 239, 278, 340, and 433 nm. The first λmax is between 239 and 282 nm. The 284–630 nm range is where the second λmax is found. The 284–630 nm range also exhibits a third λmax.

These absorption bands attest to the fact that every chemical experiences electrical excitation and absorbs UV-visible light. The compounds' perceived color is a result of light absorption and subsequent emission. As distinctive spectrum characteristics, the λmax values aid in the identification and differentiation of each constituent.

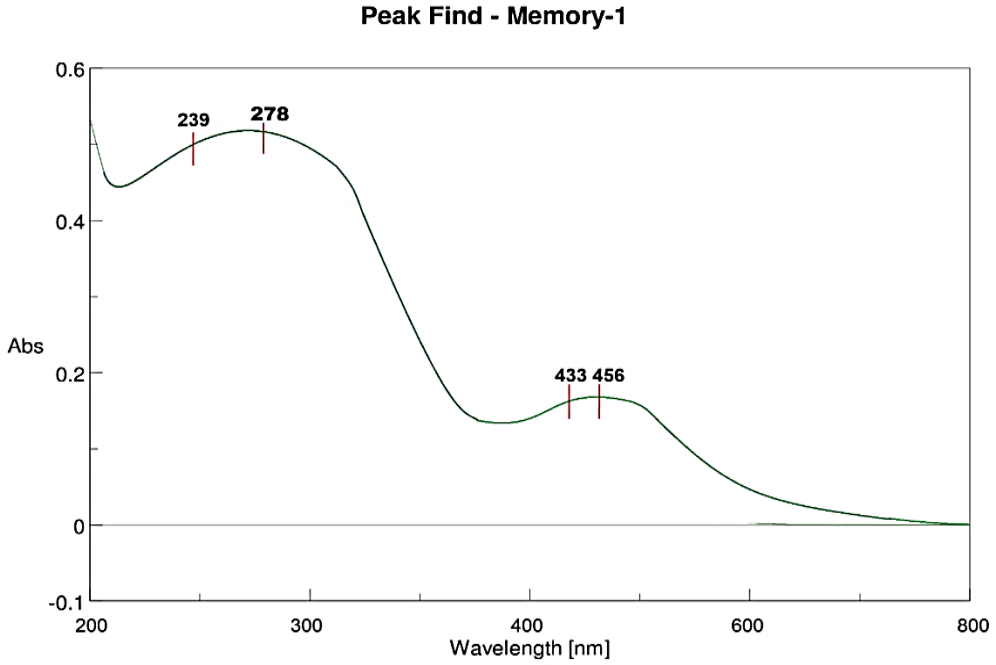

Figure9. UV spectra of CdL1

3.2.3 Elemental analysis

Cd chelate with 2 prop-2-en-1-yl N-hydroxyprop-2-ene-1-sulfinimidothioate oxime (CdL1)

The calculated carbon content is 31.00% whereas the experimental carbon content found 30.22%. Likewise, the theoretical Hydrogen content was 4.34% whereas the experimental content found as 4.11%. In case of Nitrogen, theoretical content was 6.03% whereas the experimental content found as 5.89%.

Table8. Result of Elemental analysis (CHN)

CHN analysis → Compound ↓	Carbon (%)		Hydrogen (%)		Nitrogen (%)	
	Theo.	Expt.	Theo.	Expt.	Theo.	Expt.
Cd L1	31.00	30.22	4.34	4.11	6.03	5.89

3.2.4 Mass spectroscopic study

The predicted isotopic pattern of a cadmium complex is in agreement with the experimental mass spectral data, M (464.11), M+1 (465.32), and M+2 (466.24). The readings are in close agreement with the theoretical molecular mass (464.95 g/mol), indicating that the Cd–L1 molecule was successfully formed and identified.

Table9. Molecular weights of ligand and metal complex by mass spectroscopy

Mass spectroscopic data → Compound ↓	m/z	M+1		
				M+2
Cd L1	464.95	464.11	465.32	466.24

3.2.5 Inductively Coupled Plasma–Mass Spectrometry (ICP-MS)

Cd chelate with 2-prop-2-en-1-yl N-hydroxyprop-2-ene-1-sulfinimidothioate oxime (CdL1):

The experimental cadmium content was determined to be 23.15%, whereas the theoretical cadmium content in CdL1 is 21.29%. The obtained results are very accurate for CdL1, as the percentage discrepancy between the theoretical and experimental values is less than 10%. The table's results show that the experimental and theoretical metal contents are well correlated. This demonstrates that the ICP-MS method is a reliable, accurate, sensitive, and exact way to determine the metal content of samples. All things considered, the metal content values found are acceptable and in line with theoretical predictions.

Table10. Preparation of standard linearity solutions of Cd Std

Linearity levels	Concentrations (%) w.r.t Std.	mL of stock taken	Internal Std. mL	Dilute to mL	Concentration of Cd in ppm
L1	25	0.125	1	10	0.50
L2	50	0.25	1	10	1.00
L3	100	0.50	1	10	2.00
L4	150	0.75	1	10	3.00
L5	300	1.5	1	10	6.00

Table11: Linearity data of Metal Cd

Linearity levels	Concentrations (%) w.r.t Std.	Concentration of Cd in ppm	Intensity of Cd	Correlation coefficient	R2
L1	25	0.50	21596200	0.990	1.000
L2	50	1.00	33041334		

L3	100	2.00	71170438		
L4	150	3.00	125242694		
L5	300	6.00	197995329		

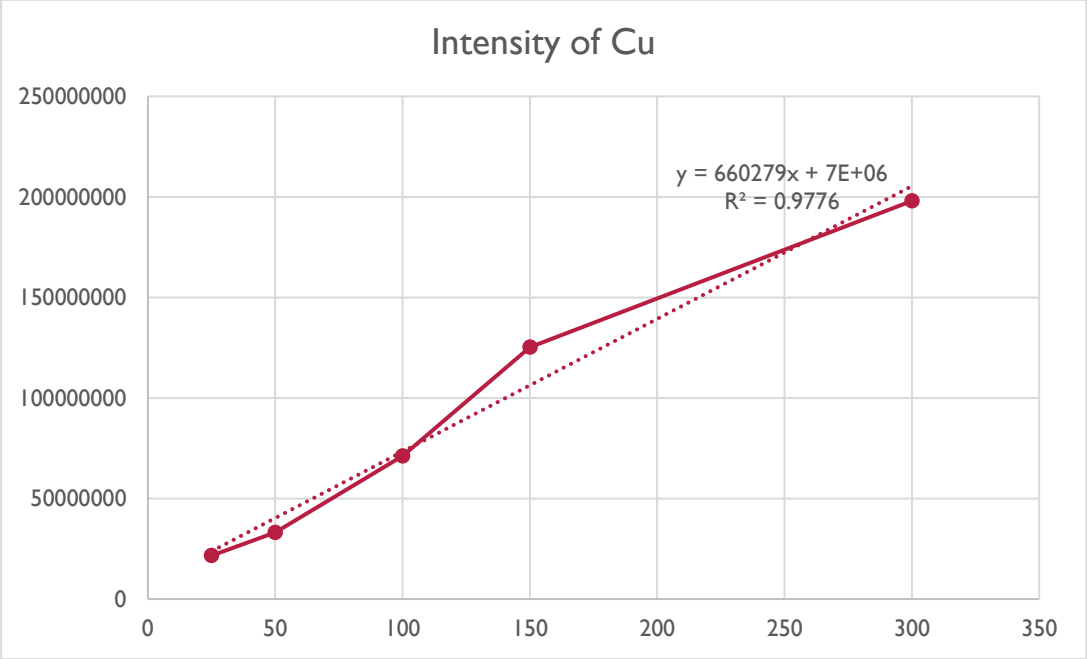

Figure10. Linearity data of Metal Cd

Table12. Result of Metal content by ICP MS

Metal content → **Compound ↓**	**% Metal content**	
	Theoretical	**Experimental**
Cd L1	21.11	22.15

3.2.6 TGA study

Thermal analysis of CdL1: Thermogravimetric measurement results for CdL1 indicated that 57.0 percent at temperature was measured at around 240^{0}C for the first time. Second weight loss at temperature 710^{0}C was observed and weight loss was observed at 90.1percent. Graphical representation shown in Figure 11

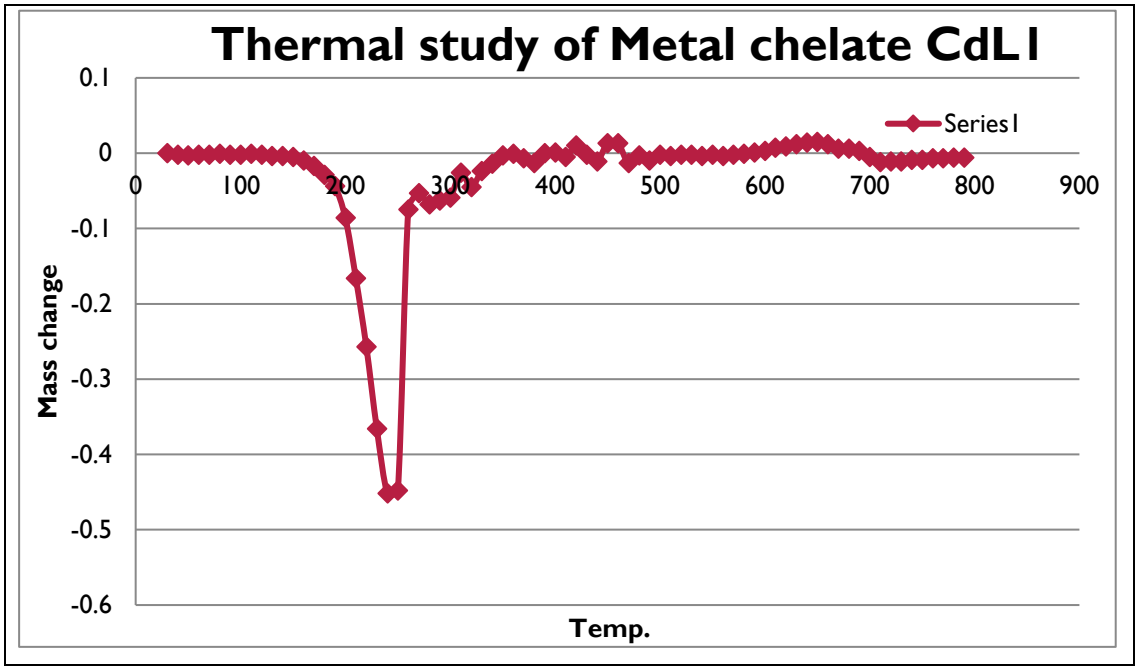

Figure11. Graphical representation of mass loss vs Temp. of CdL1

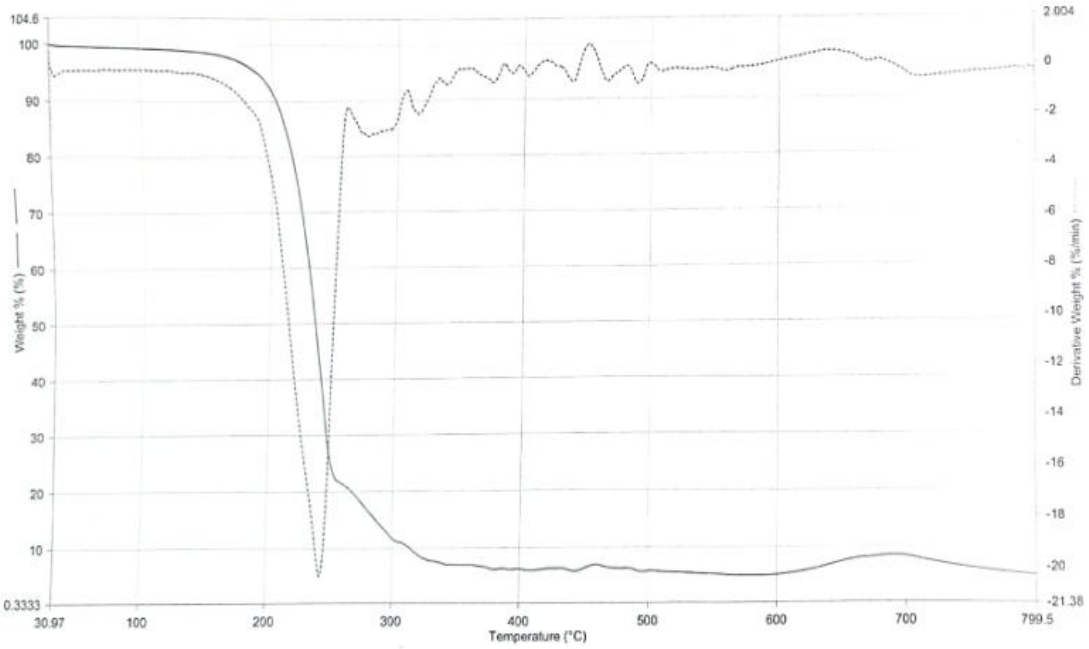

Figure12. TGA curve of CdL1

3.2.7 X-ray diffraction study

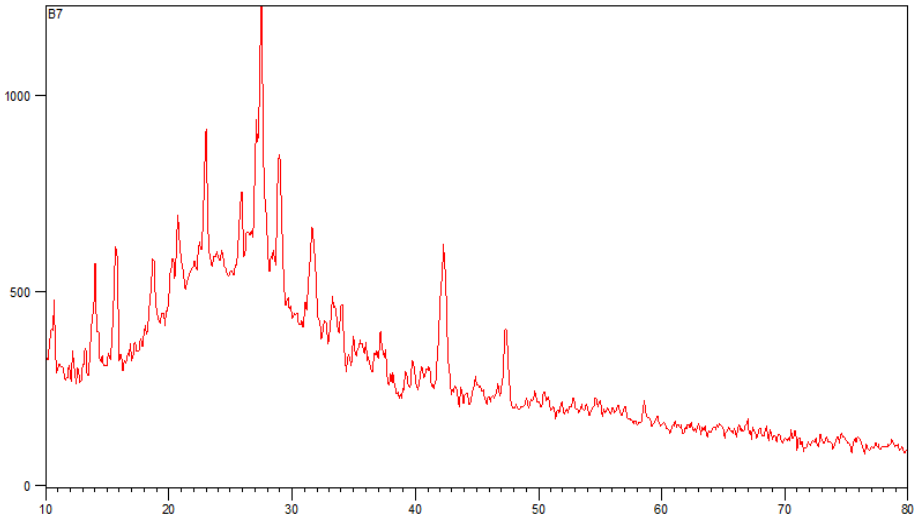

Figure13. XRD of metal chelate of CdL1

3.2.8 NMR spectroscopy

9.98–9.89 parts per million (singlet) -CHO, or aldehyde proton Aromatic aldehydes (usually 9.5–10.2 ppm) are completely matched by chemical shift. Integration appears to be about 1H. Structural implication: A fragment resembling benzaldehyde is probably present in the molecule. 7.2–8.2 ppm (complex multiplet) significant overlap between aromatic protons. Depending on the fine structure, integration seems to be between 4 and 5 H, which is compatible with either para-disubstituted or monosubstituted benzene. One aromatic ring is implied structurally. Instead of being para-substituted, the pattern seems more mono-substituted (several overlapping signals). 5.0–5.35 ppm (poor signals) Given that the shape and isolation of these tiny peaks differ from those of a real CH proton, they are most likely either residual solvent peaks (either CH_2Cl_2 or water) or minor contaminants. 3.85-3.70 ppm (small multiplets or doublets) Protons O–CH_3 or O–CH_2– Esters: 3.7–3.9 ppm O-CH_3 O-CH_2 = 3.3–3.9 ppm in ethers Implication for structure: Alkoxy or methoxy groups are suggested. 1.62–1.24 ppm (like a doublet) Methyl groups next to sp2 systems or heteroatoms: The doublet CH_3–CH: 1.0–1.6 ppm Singlet CH_3–O: 3.5 ppm (not present) These appear as doublets, indicating a single CH linked to CH_3 (~7 Hz).

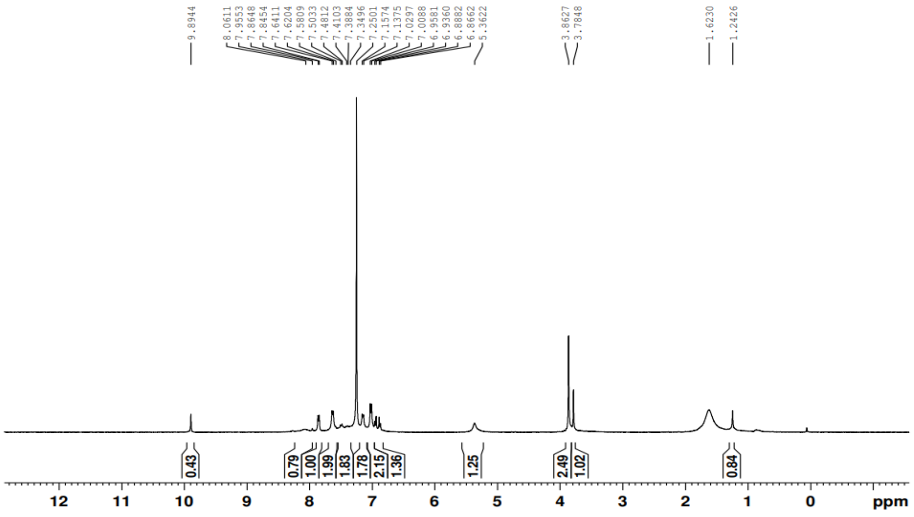

Figure14. NMR spectra of Cd chelate 2prop-2-en-1-yl N-hydroxyprop-2-ene-1-sulfinimidothioate oxime

3. CONCLUSION

The effective synthesis and thorough characterisation of transition-metal chelates made from 2-prop-2-en-1-yl-N-hydroxyprop-2-ene-1-sulfinimidothioate oxime show how well the ligand coordinates with both copper and cadmium ions.

Stable, colored crystalline complexes were produced under controlled reaction circumstances, and FT-IR, UV-Vis, NMR, mass spectrometry, CHNS elemental analysis, ICP-MS, TGA, and XRD analyses all provided solid evidence for the structures and compositions of these complexes. The suggested stoichiometries are validated and the dependability of the synthetic process is demonstrated by the strong agreement between theoretical and experimental data. Strong and distinct chelate frameworks were produced as a result of the participation of oxime and sulfinimidothioate groups in metal binding, which was further demonstrated by spectroscopic and thermal analysis. Overall, the work provides important information about the coordination chemistry, stability, and possible functional uses of sulfur–nitrogen donor metal complexes and establishes an effective and repeatable method for producing them.

Conflict of Interest

The authors have no conflict of interest to declare.

Acknowledgement

The authors express their gratitude to PES's Modern College of Pharmacy in Nigdi, Pune, for giving all the resources and assistance for the study article.

REFERENCES

[1] Wong, J.S.Y. and Wong, W.T., 2002. Synthesis, structural characterization and reactivity of triosmium carbonyl clusters containing oxime ligands. New Journal of Chemistry, 26(1), pp.94-104. https://doi.org/10.1039/B107628K

[2] Akl, M.A., Al-Awadhi, M.M. and El-Zeny, A.S., 2023. Divalent transition metal complexes of nitrogen, oxygen and sulfur containing ligand: design, structural, spectral, pH-metric, theoretical molecular modeling, analytical and mechanism studies. Applied Water Science, 13(10), p.195. https://doi.org/10.1007/s13201-023-01988-1

[3] Kukushkin, V.Y. and Pombeiro, A.J., 1999. Oxime and oximate metal complexes: unconventional synthesis and reactivity. Coordination Chemistry Reviews, 181(1), pp.147-175. https://doi.org/10.1016/S0010-8545(98)00215-X

[4] Akl, M.A., El-Asmy, A.A. and Yossef, W.M., 2005. Separation via flotation, spectrophotometric speciation, and determination of vanadium (IV) in wastes of power stations. Analytical sciences, 21(11), pp.1325-1335. https://doi.org/10.2116/analsci.21.1325

[5] Akl, M.A., Hashem, M.A., Ismail, M.A. and Abdelgalil, D.A., 2022. Novel diaminoguanidine functionalized cellulose: synthesis, characterization, adsorption characteristics and application for ICP-AES determination of copper (II), mercury (II), lead (II) and cadmium (II) from aqueous solutions. BMC chemistry, 16(1), p.65. https://doi.org/10.1186/s13065-022-00857-3

[6] Júnior, O.K., Gurgel, L.V.A., de Freitas, R.P. and Gil, L.F., 2009. Adsorption of Cu (II), Cd (II), and Pb (II) from aqueous single metal solutions by mercerized cellulose and mercerized sugarcane bagasse chemically modified with EDTA dianhydride (EDTAD). Carbohydrate Polymers, 77(3), pp.643-650. https://doi.org/10.1016/j.carbpol.2009.02.016

[7] Garcia-Sanchez, R., Bettmer, J. and Ebdon, L., 2004. Development of a new method for the separation of vanadium species and chloride interference removal using modified silica capillaries-DIN-ICP-MS. Microchemical journal, 76(1-2), pp.161-171. https://doi.org/10.1016/S0026-265X(03)00158-9

[8] Kenawy, I.M., Hafez, M.A.H., Ismail, M.A. and Hashem, M.A., 2018. Adsorption of Cu (II), Cd (II), Hg (II), Pb (II) and Zn (II) from aqueous single metal solutions by guanyl-modified cellulose. International journal of biological macromolecules, 107, pp.1538-1549. https://doi.org/10.1016/j.ijbiomac.2017.10.017

[9] Naushad, M., Ahamad, T., Alothman, Z.A. and Al-Muhtaseb, A.A.H., 2019. Green and eco-friendly nanocomposite for the removal of toxic Hg (II) metal ion from aqueous environment: adsorption kinetics & isotherm modelling. Journal of Molecular Liquids, 279, pp.1-8. https://doi.org/10.1016/j.molliq.2019.01.090

[10] Hokkanen, S., Repo, E., Suopajärvi, T., Liimatainen, H., Niinimaa, J. and Sillanpää, M., 2014. Adsorption of Ni (II), Cu (II) and Cd (II) from aqueous solutions by amino modified nanostructured microfibrillated cellulose. Cellulose, 21(3), pp.1471-1487. https://doi.org/10.1007/s10570-014-0240-4

[11] Khir, N.A.F.M., Razak, M.R.M.A., Nordin, F.J., Sofyan, N.R.F.M., Rajab, N.F. and Sarip, R., 2021. Synthesis, antiproliferative and antimalarial activities of dinuclear silver (I) complexes with triphenylphosphine and thiosemicarbazones ligands. Indonesian Journal of Chemistry, 21(3), pp.575-587. https://doi.org/10.22146/ijc.57343

[12] Wattanakanjana, Y., Janwatthana, K., Romyen, T. and Nimthong-Roldán, A., 2021. Crystal structures of copper (I) and silver (I) chloride complexes containing 4-phenylthiosemicarbazide and triphenylphosphine ligands. Asian J. Exp. Sci, 47(28), pp.10-2306. http://dx.doi.org/10.2306/scienceasia1513-1874.2021.S001

[13] Sharma, P., Nath, H., Frontera, A., Barcelo-Oliver, M., Verma, A.K., Hussain, S. and Bhattacharyya, M.K., 2021. Biologically relevant unusual cooperative assemblies and fascinating infinite crown-like supramolecular nitrate–water hosts involving guest complex cations in bipyridine and phenanthroline-based Cu (ii) coordination compounds: Antiproliferative evaluation and theoretical studies. New Journal of Chemistry, 45(18), pp.8269-8282. https://doi.org/10.1039/D1NJ01004B

[14] Dehno Khalaji, A.A., Shahsavani, E., Dusek, M., Kucerakova, M. and Eigner, V., 2020. Synthesis, Characterization, and Crystal Structures of a Thiosemicarbazone Ligand and Its Silver (I) Complex. Iranian Journal of Chemistry and Chemical Engineering, 39(4), pp.23-28. https://doi.org/10.30492/ijcce.2019.35000

[15] Anu, D., Naveen, P., Devendhiran, T., Shyamsivappan, S., Kumarasamy, K., Lin, M.C., Frampton, C.S. and Kaveri, M.V., 2021. Synthesis, spectral characterization, X-ray crystallography and biological evaluations of Pd (II) complexes containing 4 (N)-substituted thiosemicarbazone. Journal of Coordination Chemistry, 74(21-24), pp.3153-3169. https://doi.org/10.1080/00958972.2021.2025222

[16] Kotian, A., Kamat, V., Naik, K., Kokare, D.G., Kumara, K., Neratur, K.L., Kumbar, V., Bhat, K. and Revankar, V.K., 2021. 8-Hydroxyquinoline derived p-halo N4-phenyl substituted thiosemicarbazones: Crystal structures, spectral characterization and in vitro cytotoxic studies of their Co (III), Ni (II) and Cu (II) complexes. Bioorganic Chemistry, 112, p.104962. https://doi.org/10.1016/j.bioorg.2021.104962

[17] Damit, N.S.H.H., Hamid, M.H.S.A., Rahman, N.S.R.H.A., Ilias, S.N.H.H. and Keasberry, N.A., 2021. Synthesis, structural characterisation and antibacterial activities of lead (II) and some transition metal complexes derived from quinoline-2-carboxaldehyde 4-methyl-3-thiosemicarbazone. Inorganica Chimica Acta, 527, p.120557. https://doi.org/10.1016/j.ica.2021.120557

[18] Singh, N.K., Shrestha, S., Shahi, N., Choudhary, R.K., Kumbhar, A.A., Pokharel, Y. and Yadav, P., 2021. Anticancer potential of N (4) substituted 5-nitroisatin thiosemicarbazones and their copper (II) complexes. Rasayan J. Chem, 14(1600.10), p.31788. http://doi.org/10.31788/

[19] Pelagatti, P., Venturini, A., Leporati, A., Carcelli, M., Costa, M., Bacchi, A., Pelizzi, G. and Pelizzi, C., 1998. Chemoselective homogeneous hydrogenation of phenylacetylene using thiosemicarbazone and thiobenzoylhydrazone palladium (II) complexes as catalysts. Journal of the Chemical Society, Dalton Transactions, (16), pp.2715-2722. https://doi.org/10.1039/A804052D

[20] Aly, S.A. and Fathalla, S.K., 2020. Preparation, characterization of some transition metal complexes of hydrazone derivatives and their antibacterial and antioxidant activities. Arabian Journal of Chemistry, 13(2), pp.3735-3750. https://doi.org/10.1016/j.arabjc.2019.12.003

[21] Zülfikaroğlu, A., Ataol, Ç.Y., Çelikoğlu, E., Çelikoğlu, U. and İdil, Ö., 2020. New Cu (II), Co (III) and Ni (II) metal complexes based on ONO donor tridentate hydrazone: Synthesis, structural characterization, and investigation of some biological properties. Journal of Molecular Structure, 1199, p.127012. https://doi.org/10.1016/j.molstruc.2019.127012.

[22] Abouzayed, F.I., Emam, S.M. and Abouel-Enein, S.A., 2020. Synthesis, characterization and biological activity of nano-sized Co (II), Ni (II), Cu (II), Pd (II) and Ru (III) complexes of tetradentate hydrazone ligand. Journal of Molecular Structure, 1216, p.128314. https://doi.org/10.1016/j.molstruc.2020.128314

[23] Hassan, A.M., Elbialy, Z.I. and Wahdan, K.M., 2020. Synthesis, Characterization, Biological and Antitumor Activity of Co (II), Ni (II), Cu (II) and Zn (II) Complexes of N-(2-Chlorophenyl)-N′-Benzoyl Thiourea. Organic & Medicinal Chemistry International Journal, 9(3), pp.125-137. http://dx.doi.org/10.19080/OMCIJ.2020.09.555767

[24] Adjissi, L., Chafai, N., Benbouguerra, K., Kirouani, I., Hellal, A., Layaida, H., Elkolli, M., Bensouici, C. and Chafaa, S., 2022. Synthesis, characterization, DFT, antioxidant, antibacterial, pharmacokinetics and inhibition of SARS-CoV-2 main protease of some heterocyclic hydrazones. Journal of Molecular Structure, 1270, p.134005. https://doi.org/10.1016/j.molstruc.2022.134005

[25] Abkari, A., Chaabane, I. and Guidara, K., 2016. DFT (B3LYP/LanL2DZ and B3LYP/6311G+ (d, p)) comparative vibrational spectroscopic analysis of organic–inorganic compound bis (4-acetylanilinium) tetrachlorocuprate (II). Physica E: Low-dimensional Systems and Nanostructures, 81, pp.136-144. https://doi.org/10.1016/j.physe.2016.03.010

[26] Kumar, S., Devi, J. and Ghule, V.D., 2022. Synthesis, spectral analysis, DFT-assisted studies, in vitro antioxidant and antimicrobial activity of transition metal complexes of hydrazone ligands derived from 4-nitrocinnemaldehyde. Research on Chemical Intermediates, 48(8), pp.3497-3525. https://doi.org/10.1007/s11164-022-04769-8

[27] El-Tabl, A.S., Mohamed Abd El-Waheed, M., Wahba, M.A. and Abd El-Halim Abou El-Fadl, N., 2015. Synthesis, Characterization, and Anticancer Activity of New Metal Complexes Derived from 2-Hydroxy-3-(hydroxyimino)-4-oxopentan-2-ylidene) benzohydrazide. Bioinorganic chemistry and applications, 2015(1), p.126023. https://doi.org/10.1155/2015/126023

[28] Tolan, D.A., Kashar, T.I., Yoshizawa, K. and El-Nahas, A.M., 2021. Synthesis, spectral characterization, density functional theory studies, and biological screening of some transition metal complexes of a novel hydrazide–hydrazone ligand of isonicotinic acid. Applied Organometallic Chemistry, 35(6), p.e6205. https://doi.org/10.1002/aoc.6205.